Global Change Biology

Global Change Biology (2015) **21**, 1621–1633, doi: 10.1111/gcb.12800

Pyrogenic organic matter production from wildfires: a missing sink in the global carbon cycle

CRISTINA SANTÍN[1], STEFAN H. DOERR[1], CAROLINE M. PRESTON[2] and GIL GONZÁLEZ-RODRÍGUEZ[3]

[1]*Department of Geography, College of Science, Swansea University, Swansea, UK,* [2]*Pacific Forestry Centre of Natural Resources Canada, Vancouver, Canada,* [3]*Department of Statistics and Operational Research and Mathematics Didactics, University of Oviedo, Oviedo, Spain*

Abstract

Wildfires release substantial quantities of carbon (C) into the atmosphere but they also convert part of the burnt biomass into pyrogenic organic matter (PyOM). This is richer in C and, overall, more resistant to environmental degradation than the original biomass, and, therefore, PyOM production is an efficient mechanism for C sequestration. The magnitude of this C sink, however, remains poorly quantified, and current production estimates, which suggest that ~1-5% of the C affected by fire is converted to PyOM, are based on incomplete inventories. Here, we quantify, for the first time, the complete range of PyOM components found *in-situ* immediately after a typical boreal forest fire. We utilized an experimental high-intensity crown fire in a jack pine forest (*Pinus banksiana*) and carried out a detailed pre- and postfire inventory and quantification of all fuel components, and the PyOM (i.e., all visually charred, blackened materials) produced in each of them. Our results show that, overall, 27.6% of the C affected by fire was retained in PyOM (4.8 ± 0.8 t C ha^{-1}), rather than emitted to the atmosphere (12.6 ± 4.5 t C ha^{-1}). The conversion rates varied substantially between fuel components. For down wood and bark, over half of the C affected was converted to PyOM, whereas for forest floor it was only one quarter, and less than a tenth for needles. If the overall conversion rate found here were applicable to boreal wildfire in general, it would translate into a PyOM production of ~100 Tg C yr^{-1} by wildfire in the global boreal regions, more than five times the amount estimated previously. Our findings suggest that PyOM production from boreal wildfires, and potentially also from other fire-prone ecosystems, may have been underestimated and that its quantitative importance as a C sink warrants its inclusion in the global C budget estimates.

Keywords: biochar, black carbon, boreal forest, carbon emissions, charcoal, firesmart experimental fire, pyrogenic carbon

Received 21 August 2014 and accepted 16 October 2014

Introduction

Wildfires burn, on average, 464 Mha (~4%) of the Earth's vegetated land surface every year and emit 2.5 Pg of carbon (C) to the atmosphere (Randerson *et al.*, 2012), which is equivalent to a third of the current emissions from fossil fuel consumption (Boden *et al.*, 2012). The total area burned and fire intensity are projected to increase in a warming climate, which in turn will increase C emissions from wildfires (IPCC, 2013). Notwithstanding this, on the timescale of decades to centuries, wildfires are considered 'net zero C emission events', because the C emitted is balanced by C uptake by regenerating vegetation (excluding deforestation and peatland fires; Bowman *et al.*, 2009; IPCC, 2013). This 'zero C emission' scenario, however, is likely to be flawed, as it does not consider the production of pyrogenic organic matter (PyOM; also known as charcoal, 'pyrogenic carbon' or 'black carbon'). During each wildfire, instead of being emitted to the atmosphere as CO_2, other gases and as aerosols, a fraction of the burning biomass is converted to PyOM, which is a continuum from partly charred organic materials through charcoal to soot (Bird & Ascough, 2012).

PyOM is C-enriched and has an enhanced resistance to degradation, with residence times in the environment generally one or two orders of magnitude longer than its unburnt precursors (Schmidt *et al.*, 2011; Singh *et al.*, 2014). Therefore, PyOM production during wildfire could function as a long-term (decades-millennia) C sequestration mechanism (Lehmann *et al.*, 2008; Reichstein *et al.*, 2013; Ottmar, 2014). In this context, the application of 'man-made PyOM' (biochar) to soils is currently seen as one of the most viable global approaches of offsetting C emissions (Woolf *et al.*, 2010). However, despite its acknowledged importance as a C sink, the role of wildfire PyOM in the global C balance remains contentious because of uncertainties in its production and fate (Forbes *et al.*, 2006; Preston &

Correspondence: Stefan H. Doer, tel. +44 1792 295147, fax +44 1792 295955, e-mail: s.doerr@Swansea.ac.uk

Schmidt, 2006). The inclusion of PyOM in C estimates may be crucial for accurate projections of future climate change (Lehmann *et al.*, 2008) and might explain part of the elusive 'missing C sink' of ~1.5 Pg C yr^{-1} (Lal, 2008). To enable the inclusion of PyOM in C accounting, accurate quantification of the conversion of C from the fire-affected fuel (CA) to PyOM (PyC) during wildfires is required. The necessary complete quantification of the PyOM produced by wildfire, and the C retained in it (pyrogenic C, i.e., PyC), however, has never been achieved.

Previous research has pointed to a very limited proportion of the C affected by fire being converted to PyOM (~1–5%, see reviews by Preston & Schmidt, 2006 and Forbes *et al.*, 2006). The data underpinning this notion, however, are rather limited and not always representative. For example, much of the data obtained to date have been based either on laboratory experiments (e.g., Brewer *et al.*, 2013) or prescribed fires (e.g., Alexis *et al.*, 2007), which are ignited under controlled conditions for management purposes and are usually not representative of wildfire conditions (Urbanski, 2014), or on wildfires, which, because of their unpredictability, do not allow the prefire sampling of fuels (i.e., biomass, necromass and soil organic matter) necessary for calculating budgets (Forbes *et al.*, 2006). Other related research has focused on centennial-scale *in-situ* accumulation of PyOM in soils (e.g., Ohlson *et al.*, 2009; Kane *et al.*, 2010), which does not account for the fact that much of the PyOM produced is often rapidly removed from burnt sites by wind and water erosion (Santín *et al.*, 2012; Bodí *et al.*, 2014). Furthermore, some studies have only focused on specific chemically defined PyOM fractions rather than on the complete range of PyOM components (e.g., Kuhlbusch *et al.*, 1996; Czimczik *et al.*, 2003). Others have quantified PyOM in only some of the fuel components where it is produced (e.g., down wood, Donato *et al.*, 2009; aboveground fuels, Worrall *et al.*, 2013).

To achieve a complete quantification of wildfire PyOM production with respect to fuel affected by wildfire, we utilized an experimental forest fire that represented wildfire conditions. This allowed, for the first time, quantification of (i) all fuel components, and their respective C contents, before and after fire, and (ii) all the PyOM components, and their respective C contents, found *in-situ* immediately after fire.

Materials and methods

Study site and experimental forest fire

The Canadian Boreal Community FireSmart Project site is located 40 km north of Fort Providence (61°34′55″ N; 117°11′55″ W; Northwest Territories, Canada) and was also the location of the International Crown Fire Modelling Experiment (1995–2001; Stocks *et al.*, 2004). Stand-replacing fires, aimed to be representative of wildfires, are carried out here by *FPInnovations Wildfire Operations Research* in close collaboration with the NT Government to address wildfire management issues.

The experimental plot selected to be burnt was a 1.7 ha mature stand of jack pine (*Pinus banksiana*) with a tree age of 80 years, a tree density of approximately 7600 stems ha^{-1} and average tree height of 14 m. The fire was started at 16:00 hours on 23 June 2012. The ambient temperature was 28 °C and relative humidity was 22% with winds of 10–12 km h^{-1}. The last rain had occurred 6 days prior (0.5 mm), with a total precipitation over the previous month of 4.3 mm. At the time of the fire, the component values of the Canadian Forest Fire Weather Index System (Van Wagner, 1987) were: Fine Fuel Moisture Code 92.9; Duff Moisture Code 135; Drought Code 394; Initial Spread Index 9.5; Buildup Index 145 and Fire Weather Index 35. The experimental burn resulted in a high-intensity crown fire with a head fire intensity of 8000 kW m^{-1}, a flame height of 5-6 m above canopy level and a spread rate of ~6–7 m min^{-1} (Fig. 1). This fire behaviour is in the typical range for boreal crown fires (de Groot *et al.*, 2009), with the head fire intensity matching the average estimated for June in the boreal forests of Western Canada for 2001–2007 (de Groot *et al.*, 2013).

Experimental design and sampling

Before the fire, three parallel transects of 20 m length with nine sampling points each (every 2m; $n = 27$) were established in the centre of the plot in the direction of the prevailing wind (E–W). All sampling points were instrumented with thermocouples and auto-loggers (Lascar, Easylog, Wiltshire, UK) to record temperatures at the forest floor surface and at the interface between forest floor and the mineral soil (Santín *et al.*, 2013).

Fig. 1 FireSmart experimental forest fire (June 2012). This stand-replacing high-intensity crown fire (head fire intensity 8000 kW m^{-1}) reproduced typical boreal wildfire conditions (de Groot *et al.*, 2009, 2013).

A detailed prefire inventory and sampling of all fuel components: forest floor, down wood (i.e., woody debris on the ground), overstory, understory and mineral soil was carried out. Immediately after the fire (within 1–6 days), inventorying and resampling of each fuel component were repeated distinguishing between (i) remaining uncharred fuel and (ii) PyOM produced (see methodological details for each component in the following section). PyOM was visually identified, and sampled, as all blackened materials, i.e., charred, and, thus, chemically altered by fire (Bird & Ascough, 2012). This visual identification allows accounting for the whole range of the PyOM materials remaining *in-situ* immediately after the fire. Pyrogenic aerosols emitted within the smoke, and thus immediately transported *ex-situ*, are not examined in this study.

All fuel and PyOM samples were oven-dried (65 °C) and cleaned by hand to remove contamination, such as soil particles in the forest floor samples or unburnt material within the PyOM components. The dry weight of all samples was then recorded and subsamples were ground for C quantification. Total C content was determined in duplicate by quantitative high temperature combustion and conversion to CO_2 using an ANCA GSL elemental analyser interfaced with a Sercon 20/20 mass spectrometer. Presence of carbonates was tested by addition of 10% HCl to a set of representative PyOM subsamples. No effervescence was observed, what indicates a very low (<1%) concentration of carbonates (Rayment & Lyons, 2011). Therefore, the inorganic C concentration in the studied samples is considered negligible and total C as being equivalent to total organic C.

For each fuel component, mass and C loads (t ha^{-1}) in prefire fuel and postfire uncharred fuel and PyOM were calculated from field measurements, dry weights and measured C concentrations (see methodological details in the following subsection). To provide a measure of the uncertainty of our estimations (Table 1), the confidence intervals (CIs) of the estimations were derived by applying studentized bootstrap procedures for the mean (Efron, 1982). This statistical approach was chosen instead of the classical Gaussian approaches due to the asymmetry of the variables analysed and the size of the datasets, which were not large enough to balance the lack of symmetry. The studentized bootstrap CIs were thus implemented for a linear combination of independently sampled variables using the software R (version 3.1.1). All the CIs were determined at a confidence level of 95% and by using B = 10000 bootstrap iterations. Mass and C losses were calculated, for each fuel component, as the difference between prefire fuel and the remaining uncharred postfire fuel + PyOM (i.e., Fuel lost = Prefire fuel–Postfire uncharred fuel–PyOM). The conversion rate of C in fire-affected fuel (CA) to C in PyOM (PyC) was subsequently estimated (i.e., PyC/CA), with CA being the sum of PyC + C lost.

Quantification of prefire and postfire fuel and PyOM components

Detailed methodologies for quantification and sampling of the main fuel and PyOM components, pre- and postfire, are described in the following subsections.

Forest floor. Before the fire, bulk forest floor samples were taken using 20 × 20 cm sampling squares along two parallel lines between the three sampling transects (n = 10). The total depth of the forest floor was measured at each corner of the square and the entire layer was carefully collected. The forest floor was mainly composed of litter, mosses, lichens, needles, duff and humidified organic material. Cones and all woody debris <0.5 cm diameter were also considered as part of the forest floor.

After the fire, the charred forest floor layer (i.e., ash layer) and the uncharred layer underneath were sampled along the three sampling transects at every sampling point (i.e., every 2 m; n = 27). This 'charred layer' or 'ash layer' comprises both organic (i.e., PyOM) and mineral residues resulting from the burning of forest floor and aboveground inputs (Bodí *et al.*,

Table 1 Mass and C loads in fuel and pyrogenic organic matter (PyOM) components before and after fire (± bootstrap confidence intervals at 95%). PyC/CA is the conversion rate of C in fire-affected fuel (CA) to C in PyOM (PyC), with CA being the sum of PyC + C lost

			Postfire						
	Prefire		Uncharred		PyOM		Lost*		
Component	Mass (t ha^{-1})	C (t ha^{-1})	Mass (t ha^{-1})	C (t ha^{-1})	Mass (t ha^{-1})	PyC (t ha^{-1})	Mass (t ha^{-1})	C (t ha^{-1})	PyC/CA (%)
Forest floor	45.2 ± 10.3	19.7 ± 6.2	26.3 ± 3.9	9.9 ± 1.7	3.6 ± 0.6	1.9 ± 0.4	12.6 ± 8.3	6.0 ± 4.4	24.5
Down wood	38.8 ± 13.0	17.9 ± 6.0	32.7 ± 11.7	15.1 ± 5.4	1.9 ± 0.2	1.4 ± 0.2	4.0 ± 1.1	1.3 ± 0.5	51.2
Overstory									
(i) Bark	7.2 ± 3.4	3.4 ± 1.5	2.6 ± 2.1	1.2 ± 1.0	2.5 ± 1.3	1.5 ± 0.8	2.5 ± 3.2	0.8 ± 1.6	67.1
(ii) Needles	10.1 ± 1.5	5.4 ± 0.8	0.0 ± 0.0	0.0 ± 0.0	0.6 ± 0.0	0.4 ± 0.0	9.5 ± 1.5	5.1 ± 0.8	7.3
Total†	95.7 ± 15.2	42.8 ± 7.3	59.9 ± 12.2	25.3 ± 5.6	7.9 ± 1.3	4.8 ± 0.8	27.6 ± 8.7	12.6 ± 4.5	27.6

*Lost refers to what has been emitted to the atmosphere or, in the case of individual components, may include some transfer between components.

†Note that the total values have been calculated by applying studentized bootstrap procedures for the means.

2014). Wildfire ash colour can vary widely, from light to dark, depending on the fuel affected and formation conditions (Bodí *et al.*, 2014), but all ash, irrespective of its colour, is of pyrogenic origin. Therefore, in our study, all ash (even when not black) was sampled and included in our PyOM inventory.

The charred forest floor layer was sampled using a 30 × 30 cm square. The depth of the charred layer was measured at each corner of the square and the entire layer was carefully collected. For the uncharred layer beneath the charred layer, the same procedure was followed in a subsquare of 10 × 10 cm. The samples of charred forest floor were manually cleaned from any visually uncharred materials (<7% dry weight) derived from the uncharred forest floor layer underneath. The uncharred forest floor samples were cleaned of any charred particles and mineral soil (<6% dry weight). Following drying and cleaning, all samples were weighed and subsamples ground for C analyses.

Prefire mass and C loads and postfire uncharred and PyOM mass and C loads were calculated for the individual samples using their density and C contents values. Afterwards, the pre- and postfire forest floor loads (Table 1) were estimated by applying a studentized bootstrap CI for the mean on the obtained transformed samples. For calculating the lost mass and C loads (Table 1), a studentized bootstrap CI for the difference of means was used (i.e., prefire vs. postfire (uncharred + PyOM) components).

During the fire, particle traps were used to capture (and allow discounting of) any aboveground contribution to the charred layer present on the forest floor (procedure modified from Lynch *et al.*, 2004): before the fire, 17 aluminium trays (333 cm^2 each) filled with water were placed flush with the forest floor along two parallel transects at the Southern (nine trays) and Northern (eight trays) ends of the sampling transects, orientated in the direction of fire propagation. After the fire, the contents of all trays were collected by sieving (>0.2 mm) and combined to generate a composite sample. Following drying (65 °C), any uncharred material (e.g., brown needles and/or uncharred twigs and cones) was removed from this composite sample and, afterwards, its C content determined. The PyOM mass per unit area of material collected in the traps was deducted from the total production of PyOM calculated for the forest floor. The total PyOM quantified in the particle traps was assigned to the 'Overstory' component (see subsection below). This reduction in PyOM quantity for the forest floor may be somewhat too high as some of the material in the trays may have been derived from the forest floor and lifted into the particle traps by convection currents during the fire. This may result in an underestimation of the PyOM values for the forest floor. A postfire contribution to the forest floor not captured in the traps were detached small PyOM particles from charred down wood (i.e.,charcoal fragments ≤0.5 cm in size and therefore sampled as part of the postfire forest floor). It is not possible to give a reliable estimate for this potential addition. Nevertheless, the associated potential overestimation of PyOM in the forest floor component would not affect the total PyOM production estimate from this fire, as these small PyOM particles are accounted for in the forest floor, instead of the down wood component.

Down wood. Before the fire, the line intersect method (LIM) was employed to calculate loads (t ha^{-1}) of dead wood (twigs, limbs, branches and logs) on the ground (Alexander *et al.*, 2004). This involved counting the number of down wood pieces intercepting the three 20 m sampling transects (i.e. total length 60 m) using the following roundwood diameter size classes: 0.5–1.0, 1.1–3.0, 3.1–5.0 and 5.1–7.0 cm. These are referred to as Classes II-V (note that Class I, ≤0.5 diameter, is not considered in the down wood component as it was sampled and included within the forest floor). For downed logs >7.0 cm in diameter, the diameters of all pieces intersecting the transects were measured and recorded as either sound or rotten according to the degree of decay. When applying the LIM, the following standard principles were followed: trees are considered down if they lean >45°; branches still attached to standing trees are not considered; curved twigs which intersect >1 times the transect are counted at each intersection; pieces that fall perfectly in line with the transects are not tallied (Alexander *et al.*, 2004).

To calculate down wood loads Eqn (1) was used for size classes II–V:

$$W = \frac{\Pi^2 \mathrm{Gsec}(h) n QMD^2}{8L} \quad (1)$$

where W = down wood loads (t ha^{-1}), G = specific gravity (g cm^{-3}), h = piece tilt angle (degrees), n = number of intercepts over the length of the transects, QMD = quadratic mean diameter (cm), and L = length of transects (total length 60 m). The values used for G, h and QMD are those given in Nalder *et al.* (1999). For roundwood pieces >7.0 cm in diameter, Eqn (2) was used to calculate loads:

$$W = \frac{\Pi^2 \sum d^2 G}{8L} \quad (2)$$

where W = down wood loads (t ha^{-1}), Σd^2 = sum of the squared diameters for intercept pieces (cm^2), G = specific gravity (g cm^{-3}) with different values for sound and rotten pieces according to Delisle & Woodard (1988), and L = length of transects (total length 60 m). The moisture content of rotten pieces >7.0 cm before the fire was too high for ignition. They were therefore excluded from postfire calculations.

According to Eqns (1) and (2), the contribution to W of each down wood piece intercepting the sampling transects can be computed in such a way that W is the sum of the individual contributions. Using these individual contributions, a studentized bootstrap for the total W (with the mean adjusted by the sample size) was applied to estimate total prefire mass loads in Table 1. Subsequently, to estimate total prefire C loads (Table 1), the mass of each individual contributions (i.e., pieces) was multiplied by the C content of representative down wood samples (Table 2), and, in the same way as for mass loads, a studentized bootstrap for the total was applied.

After the fire, the LIM was repeated. The accurate relocation of the transects was facilitated by metal pins placed prior to the fire. During postfire sampling, we observed an increase in the number of down wood pieces for some size classes compared to prefire values (e.g., for size class IV a total of 18 pieces were detected along the three transects before the fire and 29 after the fire). This is likely due to removal of the upper

Table 2 Average C concentrations in prefire fuels and postfire uncharred fuels and PyOM. Values are given as the arithmetic mean ± standard error of the mean, number of samples is given in brackets

		Postfire	
	Prefire	Uncharred	PyOM
Component	C (g g sample^{-1})	C (g g sample^{-1})	C (g g sample^{-1})
Forest floor	0.405 ± 0.020 (10)	0.369 ± 0.020 (27)	0.541 ± 0.020 (27)
Down wood	0.462 ± 0.000 (3)	*0.462 ± 0.000 (3)	0.729 ± 0.038 (3)
Overstory			
(i) Bark	0.473 ± 0.017 (10)	*0.473 ± 0.017 (10)	0.629 ± 0.012 (10)
(ii) Needles	0.544 ± 0.010 (8)	n.a.	0.680 ± 0.002 (6)

*Prefire values are used; n.a.: not applicable.

part of the forest floor by fire exposing previously embedded, and hence not recorded, down wood (Volkova & Weston, 2013). These 'buried pieces' are not accounted for in down wood inventories (Brown, 1974). To overcome this postfire shortcoming of the LIM method, we used the following alternative sampling approach for determining the amounts of PyOM produced from the down wood component: a representative initial area of 40 m^2 was selected 20 m east of the experimental transects, and all down wood pieces present after the fire were examined. For each piece, its diameter was recorded and the depth of charring measured, both on the side with the deepest charring depth and the opposite side. Pieces were either broken or sawn in half to measure charring depth. For size classes IV and above, the sampling area examined was increased to reach a minimum of 60 pieces for each size class. From these data, an average charring depth was assigned to each size class (note that size class I was not examined as it was sampled and included within the forest floor component).

After the fire there was no evidence of log trenches or shallows, which are indicators of complete combustion (Tinker & Knight, 2000). Hence it was reasonable to assume no complete combustion occurred for the larger classes (>3 cm diameter). Complete or nearly-complete combustion of smaller size classes may have occurred, but any small PyOM particles (≤0.5 cm diameter) remaining on site from these would have been sampled as part of the forest floor. No standing trees fell during or immediately after the fire, so contribution from standing trees to down wood was considered to be zero.

The postfire PyOM loads in down wood (Table 1) were estimated as for the prefire mass loads (i.e., studentized bootstrap for the total), but taking into account the measured mean charring depth for each size class (instead of total diameters) as well as a G value of 0.23 g cm^{-3} (±0.02 SEM-standard error of the mean) obtained from representative charred down wood samples collected in the field (n = 13). C loads in PyOM (Table 1) were then calculated by multiplying PyOM mass loads in each class size by the measured C content of representative charred down wood samples (Table 2) and computing again a studentized bootstrap CI estimation. For estimates of the proportion of down wood that had been lost during combustion (Table 1) we used the average proportions of 8.8% for coarse down wood (>7 cm diameter) and 16.1% for fine down wood (<7 cm diameter), with respect to prefire loads, measured during an experimental fire of similar characteristics (head fire intensity ~8000 kW m^{-1}) in a mature jack pine stand (Stocks, 1989) and the corresponding studentized bootstrap CIs. Subsequently, total uncharred down wood remaining after the fire was estimated by applying a studentized bootstrap CI to the difference between prefire down wood and down wood converted to PyOM + down wood lost (note that all of these measurements are performed on the same individuals). C loads in the postfire uncharred downwood were calculated in the same way as the prefire C loads, i.e., by multiplying each uncharred mass individual contribution by the C content of representative uncharred (prefire) downwood samples (Table 2), and by applying a studentized bootstrap for the total (Table 1). Finally, the C lost was calculated by computing a studentized bootstrap mean CI to the difference between C in the prefire down wood and C remaining in postfire uncharred down wood + C in PyOM (note that also these calculations are applied on the same individuals).

Overstory. To calculate tree density, overstory trees (i.e., trees with a Diameter at Breast Height measured Outside the Bark (DBHOB) >3.0 cm) were inventoried using the point-centred quarter method (Alexander *et al*., 2004). This involved measuring the distance from each sampling point (i.e., every 2 m along the three sampling transects) to the nearest tree in each of the four quarters of an imaginary square, the centre of which is the sampling point. In addition, for each tree, the species and condition (live or dead) were recorded and the DBHOB measured. If in a given quarter there was no tree <5 m from the centre, that quarter was recorded as 'no tree', and, when calculating tree density, established correction factors were applied (Mitchell, 2007).

Tree density (0.76 stems m^{-2}) was calculated following Eqn (3):

$$D = \frac{1}{\sqrt{AD}} \tag{3}$$

where D = overstory tree density (number of stems m^{-2}), and AD is the average distance (m) from the closest tree to the sampling point (i.e., 1.60 m ± 0.09 SEM; n = 108).

All trees were killed by the fire but none fell during or immediately after the fire so total tree density pre- and postfire was considered to be the same.

Overstory I: stems—Standing tree stems suffered almost exclusively only charring of the bark. Evidence of wood charring was only detected in some pre-existing snags. Therefore, we focused on bark as the main component for PyOM production from stems. Before the fire, bark was sampled from representative trees (n = 10) outside the sampling area so that bark sampling did not affect fire behaviour within the burnt plot. For each tree, DBHOB and height was recorded and the entire bark layer was scraped at breast height from an area of 20 cm height around the whole trunk (i.e., a 20 cm strip of bark taken at +/− 10 cm from DBHOB height). After the fire, bark was sampled at representative trees (n = 10) within the three experimental transects using the same procedure as before the fire, but with separating the charred and the uncharred layers of bark. The sampled trees were subsequently felled to facilitate recording of (i) total tree charring height and (ii) fire effects on the canopy (i.e., needles and branches). Total tree height and DBHOB were also recorded. Bark samples (prefire and postfire charred and uncharred) were oven dried (65 °C), weighed and a subsample ground for C analyses.

Total prefire bark mass per tree was estimated by multiplying the measured mass of bark (g m^{-2}) by the total tree surface area (m^2) calculated by assuming a conical tree shape. The estimated total bark mass per tree was multiplied by the average total tree density in the experimental plot (0.76 stems m^{-2}) to obtain an estimation of prefire bark loads (t ha^{-1}) based on each sampled tree. The final bark load estimation (Table 1) was obtained by applying a studentized bootstrap CI mean estimation on the obtained transformed sample. Similar calculations for postfire sampled trees were done, distinguishing between the charred and uncharred bark mass per tree by using the total height as well as the height of charring. In our approach, we assume homogeneous charring of the bark along the whole height of charring, although it is conceivable that the charring degree of the bark varies along the trunk, with deeper charring at the base of the tree, where the bark is in contact with ground fuels.

To obtain prefire bark C loads, the C content in bark measured for each prefire tree was multiplied by the corresponding total dry prefire bark load estimation. For postfire charred bark (PyOM) the same procedure was applied by using the C content measured for each postfire sample, and distinguishing between charred and uncharred bark (for uncharred bark the average C content value for prefire bark was used, see Table 2). As before, the final total estimation (Table 1) was obtained by applying a studentized bootstrap CI mean estimation on each obtained transformed C sample. Finally, 'lost bark mass' (Table 1) was computed by applying a studentized bootstrap CI for the difference of means for independent samples [i.e., prefire mass vs. postfire (charred + uncharred) mass]. An analogous procedure was applied for estimating 'lost bark C' [prefire C vs. postfire (charred + uncharred) C].

Overstory II: canopy—For the type of forest fire investigated here, crown fuels are commonly considered to be limited to needles and dead branchwood material <1 cm diameter (Stocks, 1989). Visual examination of the felled trees showed that needles were the principal crown component burnt whereas branches and twigs suffered minimal charring. Therefore, only needle loads were considered when accounting for PyOM production from the canopy. Prefire needle fuel loads were derived using the regression Eqn (4) developed for this experimental site during the International Crown Fire Modelling Experiment (Alexander *et al.*, 2004):

$$Y = 0.00672X^{2.25699} \quad (4)$$

where Y is total dry needle weight (kg) and X is DBHOB.

Needle fuel loads were calculated according to this equation for each (live) tree for which DBHOB had been measured for the calculations of 'overstory tree density' described at the beginning of the 'Overstory' subsection (n = 38). Needle weights were then converted to loads (t ha^{-1}) using the (live) tree density in the experimental plot (0.40 stems m^{-2}) and a studentized bootstrap CI for the mean was applied (Table 1). C loads were then calculated by multiplying the total needle loads by the C content determined from fresh needle samples (Table 2) and, as before, a studentized bootstrap CI for the mean was applied (Table 1). After the fire, only a few needles remained in the trees, which were dead, but not charred (i.e., brown due to heat, but not chemically altered by the fire). For calculations (Table 1), we therefore assumed that essentially no needles remained in the crown after the fire (either charred or uncharred). Thus, any PyOM produced from needles either fell on the ground or was lost from the system, i.e., transported *ex-situ* within smoke during fire. To estimate the PyOM production from this component, the PyOM quantified in the particle traps placed on the forest floor was entirely attributed to canopy contribution (see 'Forest Floor' subsection above). It is conceivable that the material captured in the trays also included a contribution from charred bark from standing stems and, as stated before, also particles lifted from the forest floor by convection currents during the fire. Thus, the *in-situ* PyOM deposition from needles estimated here is probably an overestimate of the aboveground contribution, but will not affect the total PyOM production estimate.

Understory. Before the fire, the understory inventory involved recording the diameters at breast and ground height (cm) and the height (cm) of any understory stems (i.e., saplings and shrubs <3.0 cm DBHOB) at every sampling point along each transect using a 1 m radius fixed plot (Alexander *et al.*, 2004). Understory vegetation, however, was so scarce (<0.1 stems m^{-2}) that this component was considered irrelevant and not further included in this study.

Mineral soil. Before the fire, bulk samples of the mineral soil were taken using a 5 × 5 cm soil corer (n = 10) along two

parallel lines between the three sampling transects, at the same sampling points as for the prefire forest floor sampling. The mineral soil sampled was a waterlogged, stony sandy loam derived from fluvio-glacial deposits. The fire did not affect the mineral soil (maximum temperature recorded at mineral soil surface was <70 °C, n = 27). Therefore, soil was not a relevant fuel component for this study and not further considered.

Results

Forest floor

The forest floor had an average depth to the mineral soil of 6.5 cm (±0.3 SEM; n = 108) and is the studied fuel component storing the largest amount of C before the fire (19.7 ± 6.2 t ha^{-1}, Table 1). During the fire, the mean maximum temperature at the surface of the forest floor was 750 °C (range 550–976 °C, n = 27) with a mean residence time >300 °C of 180 s (range 65–365 s) (see Santín *et al.*, 2013 for further details). This resulted in an average charring depth of the forest floor of 3.9 cm (±0.2 SEM; n = 108) and generated a continuous layer of charred material, i.e. ash (1.3 cm avg. depth ± 0.1 SEM; n = 108) (Fig. 2). This charred layer is C enriched (0.541 ± 0.020 g g^{-1}) compared both to the prefire forest floor (0.405 ± 0.020 g g^{-1}) and the postfire uncharred layer (0.369 ± 0.020 g g^{-1}; Table 2). Overall, 1.9 ± 0.4 t C ha^{-1} were converted to PyOM within the forest floor, whereas 6.0 ± 4.4 t ha^{-1} were lost (i.e., potentially emitted to the atmosphere) (Table 1). This translates into a conversion rate of 24.5% PyC/CA for the forest floor. It is important to note, as is common for boreal forest wildfires (de Groot *et al.*, 2009), that only the upper part of the forest floor was affected by fire; i.e., only 42% of the total prefire fuel load (19.7 ± 6.2 t ha^{-1}, Table 1).

Down wood

Prefire down wood loads were high (38.8 ± 13.0 t ha^{-1}, Table 1), with the greatest contribution being from the bigger size classes: 0.69 t ha^{-1} (class II), 1.38 t ha^{-1} (class III), 2.66 t ha^{-1} (class IV), 4.01 t ha^{-1} (class V), 27.30 t ha^{-1} (>7 cm, sound) and 2.91 t ha^{-1} (>7 cm, rotten). However, the smallest down wood pieces were those most affected by fire, showing average charring depths of 2.60 mm (±0.05 SEM, n = 122) for size class II and 8.10 mm (±0.03 SEM; n = 85) for size class III. None of the thicker pieces (classes IV and above) were completely carbonized, with average charred depths of 1.86 mm (±0.20 SEM; n = 60) and 1.89 mm (±0.25 SEM; n = 60) for classes IV and V, respectively. For coarse woody debris (i.e. >7 cm diameter, sound), the charring was even shallower [0.86 mm (±0.13 SEM; n = 60)].

Overall, 32.7 ± 11.7 t ha^{-1} of the down wood mass remained unaffected by the fire, 1.9 ± 0.2 t ha^{-1} of the down wood was converted into PyOM and 4.0 ± 0.2 t ha^{-1} was lost (Table 1). The PyC/CA rate for the down wood component was 51.2% (Table 1, Figure 2), twice that obtained for the forest floor. Down wood PyOM showed the greatest C enrichment of all fuel components compared to the unburnt precursors, from 0.462 ± 0.00 to 0.729 ± 0.038 g g^{-1} (Table 2).

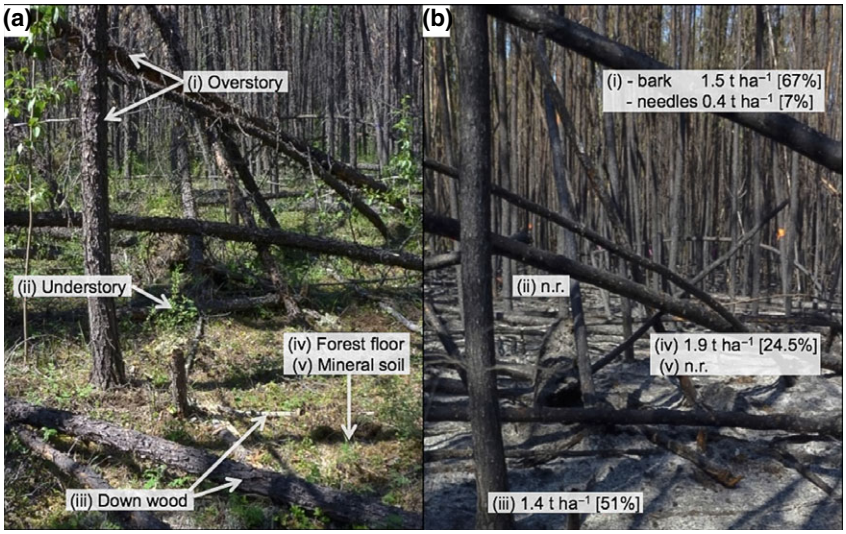

Fig. 2 The FireSmart experimental forest fire enabled prefire (a) and immediate postfire (b) inventory and sampling of fuel components (i–v in a), and of their respective amounts of pyrogenic organic matter produced (i–v in b). Pyrogenic organic matter production is given for each of the fuel components in t C ha^{-1}, and also as the ratio of C converted to pyrogenic organic matter with respect to C affected by fire [%] (see Table 1 for more details). n.r.: not relevant in this fire.

Overstory

The total prefire loads estimated for the overstory component are not equivalent to total tree biomass because they do not include the standing timber, which was not affected by fire. Prefire loads for needles (10.1 ± 1.5 t ha^{-1}) were higher than for bark (7.2 ± 3.4 t ha^{-1}) (Table 1), however, the PyOM production was much higher for bark than for needles, both in terms of total amounts of C (1.5 ± 0.8 and 0.4 ± 0.0 t PyC ha^{-}, respectively) and as PyC/CA rate (67.1% and 7.3%, respectively) (Table 1, Fig. 2). C enrichment in PyOM for needles involved an increase from 0.544 ± 0.01 to 0.680 ± 0.002 g g^{-1} and for bark from 0.473 ± 0.017 to 0.629 ± 0.012 g g^{-1} (Table 2).

Discussion

This typical boreal forest fire produced 7.9 ± 1.3 t ha^{-1} of PyOM (containing 4.8 ± 0.8 t PyC ha^{-1}) and converted 27.6% of the CA to PyC (Table 1). The three main fuel components, i.e., forest floor, down wood and overstory (bark and needles combined), produced broadly similar amounts of PyC (1.9 ± 0.4, 1.4 ± 0.2 and 1.9 ± 0.8 t ha^{-1} respectively; Table 1). The PyC/CA conversion rates, however, show substantial differences. For down wood and bark, over half of the CA was converted to PyC whereas for forest floor, only a quarter of the CA was converted to PyC. For needles only 7% of the CA was converted to PyC, with the rest having been combusted, which is broadly in agreement with the assumptions of complete combustion of previous studies (Knorr *et al*., 2012). Needles and forest floor materials have a much higher surface area to volume ratio than tree stems (bark) and down wood, facilitating access to oxygen and hence greater combustion completeness, resulting in lower PyC/CA conversion for the fuel components with relatively high surface areas (Kuhlbusch & Crutzen, 1995). The lower combustion completeness of fuel with a low surface area to volume ratio is also reflected in the greater relative C enrichment of the PyOM produced within these fuel components (Table 2). This lower combustion completeness could be also related to the different chemical composition of the fuel components, with materials richer in lignin such as pine wood (Räisänen & Athanassiadis, 2013) suffering relatively smaller mass losses during charring (Czimczik *et al*., 2002; Cornwell *et al*., 2009).

The overall PyC/CA conversion rate of 27.6% found here is substantially higher than previous estimates for boreal regions and other ecosystems elsewhere (~1–5% PyC/CA; reviews by Kuhlbusch & Crutzen, 1996; Forbes *et al*., 2006; Preston & Schmidt, 2006). Table 3 summarizes the outcomes of 31 studies quantifying PyOM production in different ecosystems and using various approaches. We suggest three main reasons for the substantially lower estimations in these previous studies.

Firstly, most previous approaches have accounted for only some of the PyOM components formed *in situ* during fire. For instance, in the same forest complex investigated here, a 2% fuel mass conversion to PyOM was reported for a fire from the International Crown Fire Modelling Experiment (Lynch *et al*., 2004). However, that investigation only accounted for airborne PyOM collected in particle traps. It, therefore, excluded PyOM formed from, and remaining within, the forest floor, down wood and bark on standing trees. As another example, Fearnside *et al*. (2001) estimated a 6% PyC/CA conversion for a prescribed fire in the Amazonian rainforest, but they only accounted for woody charcoal pieces collected manually from the ground. They thus excluded, amongst others, the PyOM contained in fine residues (e.g., ash, charred forest floor or litter), which can be a substantial pool of PyC (Santín *et al*., 2012).

Secondly, the use of analytical approaches that quantify only a part of the PyOM continuum can lead to underestimation if the values obtained are assumed to represent the total PyOM produced. For example, Kuhlbusch *et al*. (1996) estimated a PyC/CA conversion rate of only 0.6–1.5% during an open-tree Savanna experimental fire, but this was done using a chemical/thermal oxidation method that quantifies only the most condensed forms of PyOM (Schmidt *et al*., 2001).

Thirdly, some studies used prescribed burns, which are usually not representative of wildfires, and sometimes carried out in human-manipulated fuels (Urbanski, 2014). For example, Fearnside, Gráça and collaborators have carried out several PyOM production inventories for tropical slash-and-burn fires (see details in Table 3). Slash-and-burn fires are aimed at maximizing fuel consumption, resulting in high combustion completeness and, therefore, lower rates of PyOM production compared to wildfires (Kuhlbusch & Crutzen, 1995). It is worth highlighting here that, in their latest and most comprehensive study, they estimated a PyC/CA conversion rate of 16% (Righi *et al*., 2009), which is substantially higher than their earlier, and less complete, estimations (Table 3: Fearnside *et al*., 1993, 1999, 2001, 2007; Gráça *et al*., 1999).

Our study overcomes the limitations outlined above as we (i) quantified PyOM produced in all fuel components; (ii) included the entire range of PyOM materials and (iii) examined a forest fire representative of typical wildfire conditions. To the authors' knowledge, it therefore represents the most comprehensive quantification to date of PyOM produced *in situ* during a wildfire. Whilst drawing general conclusions from a single fire

Table 3 Previous estimates of pyrogenic organic matter (PyOM) production from wildfires, prescribed and experimental fires. PyOM production is given as the ratio of C converted to PyOM (PyC) with respect to C affected by fire (CA) [% PyC/CA], and as the quantity of PyC produced (t PyC ha^{-1}). Not included are studies (i) focusing on long-term PyOM pools, (ii) summarizing previous work on PyOM production and (iii) those dealing with atmospheric black carbon or biochar

Study	Ecosystem	Type of fire	PyOM production [%PyC/CA (t PyC ha^{-1})]	PyOM component(s) studied	PyOM detection and quantification††
Clark *et al.*, 1998	Boreal‡‡	Experimental (wildfire)	2 (0.7)*	Airbone particles	Visual & gravimetric
Czimczik *et al.*, 2003	Boreal‡‡	Wildfire	0.7 (0.06)†	Forest floor	Molecular markers (Benzenopolycarboxylic acids)
Lynch *et al.*, 2004	Boreal‡‡	Experimental (wildfire)	2 (0.58)*	Airbone particles	Visual & gravimetric
Makoto *et al.*, 2012	Boreal‡‡	Wildfire	n.d. (0.25–0.06)*	Bark on standing snags	Visual & gravimetric
Ohlson & Tryterud, 2000	Boreal‡‡	Experimental (wildfire)	n.d. (0.23)*	Airbone particles	Visual & gravimetric
Pitkänen *et al.*, 1999	Boreal§§	Prescribed (slash-and-burn)	n.d. (1.4)*	Airbone particles	Visual & gravimetric
Brewer *et al.*, 2013	Temperate‡‡	Laboratory (fuel beds)	7.2–8.7 (2.0–2.5)	All fuels selected	Visual, gravimetric & total C quantification
Finkral *et al.*, 2012	Temperate‡‡	Prescribed (slash pile)	1–5 (0.05–0.21)	All	Visual, gravimetric & total C quantification
Pingree *et al.*, 2012	Temperate‡‡	Wildfire & prescribed	‡1–8 (n.d.)	Soil§	Chemical (peroxide-acid digestion) & C quantification
Tinker & Knight, 2000	Temperate‡‡	Wildfire	*50 (6.4)	Coarse down wood	Visual & volumetric
Eckmeier *et al.*, 2007	Temperate§§	Experimental (slash-and-burn)	8.4 (5.4)	All (>1 mm)	Visual, gravimetric & total C quantification
Aponte *et al.*, 2014	Temperate***	Prescribed (several)	n.d. (0.22–0.33)	Coarse down wood**	Visual, volumetric & total C quantification
Santín *et al.*, 2012	Temperate***	Wildfire	n.d. (3.6–9.7)	Ash	Organic C quantification
Clay & Worrall, 2011	Temperate†††	Wildfire	4.3 (0.12)	Aboveground excl. standing wood	Visual, gravimetric & total C quantification
Worrall *et al.*, 2013	Temperate†††	Prescribed	2.6 (n.d.)	Aboveground excl. standing wood	Visual, gravimetric & total C quantification
Fearnside *et al.*, 1993	Tropical‡‡‡	Prescribed (slash-and-burn)	2.7 (n.d.)†	All but fine residues	Visual & gravimetric
Fearnside *et al.*, 1999	Tropical‡‡‡	Prescribed (slash-and-burn)	2.9 (2.2)	All but fine residues	Visual & gravimetric
Fearnside *et al.*, 2001	Tropical‡‡‡	Prescribed (slash-and-burn)	5.8 (3.2)	All but fine residues	Visual & gravimetric
Fearnside *et al.*, 2007	Tropical‡‡‡	Prescribed (slash-and-burn)	4.0 (1.2)	All	Visual & gravimetric
Gráça *et al.*, 1999	Tropical‡‡‡	Experimental (slash-and-burn)	8.4 (4.5)	All	Visual, gravimetric & total C quantification
Kauffman *et al.*, 1995	Tropical‡‡‡	Prescribed (slash-and-burn)	1.4–5.3 (1.4–3.1)	Ash	Total C quantification
Carvalho *et al.*, 2011	Tropical§§§	Prescribed	0–6.2 (n.d.)*	Experimental (wood blocks)	Visual & gravimetric
Kauffman *et al.*, 1998	Tropical****	Prescribed (slash-and-burn)	3.7–4.8 (0.5–0.8)	Ash	Total C quantification
Righi *et al.*, 2009	Tropical††††	Prescribed (slash-and-burn)	16.2 (6.0)	All	Visual, gravimetric & total C quantification

Table 3 (continued)

Study	Ecosystem	Type of fire	PyOM production [%PyC/CA (t PyC ha^{-1})]	PyOM component(s) studied	PyOM detection and quantification††
Rumpel *et al.*, 2009;	Savanna‡‡‡‡	Prescribed (slash-and-burn)	0.4 (0.48)†	All	Visual, gravimetric & total C quantification
Kuhlbusch *et al.*, 1996;	Savanna§§§§	Experimental (slash-and-burn)	0.6–1.5 (<0.05)	All	Thermo-chemical & C quantification
Saiz *et al.*, 2014;	Savanna‡‡‡‡′§§§§	Experimental (1 m^2 plots)	11–23 (0.23–1.24)†	Surface fuels excl. coarse DW	Visual & gravimetric& total C quantification
Donato *et al.*, 2009;	Mediterranean‡‡	Wildfire	n.d. (0.3–0.6)	Down wood	Visual & volumetric
Goforth *et al.*, 2005;	Mediterranean‡‡′ §§	Wildfire	n.d. (1.15–1.45)	Ash	Organic C quantification
Alexis *et al.*, 2007;	Mediterranean*****	Prescribed	5.4 (1.4)	All	Visual, gravimetric & total C quantification
Kuhlbusch & Crutzen, 1995	Various	Laboratory (burning apparatus)	0.1–3.4 (n.d.)	All fuels selected	Thermo-chemical & C quantification

*Values given in relation to total mass consumed.
†Values given in relation to prefire total C.
‡Values given in relation to woody fuel mass consumed.
§Postfire sampling 1–2 year after fire without accounting for losses due to postfire erosion.
**Postfire sampling 4–7 year after last fire.
††Unless stated otherwise C quantification was not performed and C values (where reported) were obtained from previous studies.
‡‡Conifer fores.
§§Deciduous forest.
***Eucalyptus forest.
†††Moorland.
‡‡‡Humid rainforest.
§§§Seasonal conifer.
****Seasonal grassland.
††††Seasonal semideciduous.
‡‡‡‡Grassland.
§§§§Open-tree grassland.
*****Scrub oak.
n.d.: not determined.

event, as that investigated here, must be done with caution, our results highlight a likely underestimation of PyOM production in previous studies of boreal forests and also beyond.

The boreal forest represents the world's largest terrestrial biome and contains >30% of terrestrial C stock (Kelly *et al*., 2013), with wildfire being a dominant driver of the C balance here (Bond-Lamberty *et al*., 2007). Currently, 12.4 Mha of boreal regions burn on average each year and climate change is expected to lead to a substantial increase in wildfire season severity (Flannigan *et al*., 2013). There is already evidence that recent changes in climate have already lengthened the fire season in the North American boreal forest (Kelly *et al*., 2013). As our fire was typical for wildfires in the surrounding boreal region, it may be informative to scale up by combining the overall PyC/CA conversion rate from this study with global estimates for boreal regions of average fuel consumption (g C per m^2 of area burnt; Van der Werf *et al*., 2010) and area burnt (Mha yr^{-1}; Randerson *et al*., 2012). This gives a PyC production estimate within boreal regions of ~100 Tg yr^{-1}, which is more than five times higher than the previous estimates of 7–17 Tg yr^{-1} (Preston & Schmidt, 2006). Although this scaling up is rather speculative and the representativeness of the conversion rate found here for boreal forest fires needs to be validated more widely, this outcome suggests that boreal PyC production could represent a substantial C sink at the global scale.

The ability of PyOM to act as a C sink in the long-term is conditioned by its longevity in the environment. It is therefore important to recognize that, even if the overall resistance to degradation of PyOM is higher than its unburnt precursors (Schmidt *et al*., 2011) and some PyOM forms can persist in the environment for millennia, others can be mineralized relatively fast (within days or months) (Singh *et al*., 2012; Zimmerman *et al*., 2012). The longevity of PyOM depends on both its intrinsic resistance to degradation (mainly driven by fuel properties and burning conditions, e.g., Soucémarianadin *et al*., 2013) and on the characteristics of the environment itself (e.g., oxygen availability, physical protection; Marschner *et al*., 2008; Singh *et al*., 2014). Therefore, for a complete quantitative assessment of the C sequestration potential of wildfire PyOM, an evaluation of the resistance to degradation of the different forms of PyOM is also required. In boreal regions, a particularly long half-life in the range of hundreds or thousands of years can be expected for the most recalcitrant PyOM fractions, because of specific formation and environmental conditions (e.g. relatively high production temperatures and cool climate) (Preston & Schmidt, 2006).

Given the overall importance of the boreal biome in the global C balance, the finding that nearly a third of the C in boreal biomass affected by wildfire could be transformed into PyOM rather than emitted to the atmosphere is significant. The inclusion of wildfire PyOM production, and its C sequestration potential, in C budgets would, therefore, be an important step in reducing the uncertainty in C accounting and, thus, future climate projections (Lehmann *et al*., 2008). At present, C cycle uncertainties are among the major unknowns affecting scenario development (Moss *et al*., 2010) and wildfires are one of the environmental perturbations least understood in terms of their impact on the global C cycle (Reichstein *et al*., 2013). Although our study is focused on the boreal region, we have identified a previous general underestimation of PyOM production from wildfire studies that applies, to some extent, also to other major fire-prone ecosystems (Table 3). Further research, including the comprehensive quantification of PyOM production for a range of ecosystems and fire behaviours, as well as the longevity in the environment of the different forms of PyOM, is required to fully address the role of PyOM in the global C budget.

Acknowledgements

C.S. is grateful to the Spanish Ministry for a mobility postdoctoral fellowship (EX2010–0498) and to the University of Oviedo (Spain), her previous affiliation. Fieldwork was supported by the College of Science of Swansea University via a Research Fund disbursal exercise. Funding by the The Leverhulme Trust (Grant RPG-2014-095) enabled data analysis and manuscript preparation. Special thanks go to Ray Ault (FP-Innovations), and Larry Nixon and Danny Beaulieu (Environment and Natural Resources, GNT) for enabling us to participate in the FireSmart project. Thanks also to Stephanie Koroscil (Univ. of Alberta), the staff of FP-Innovations, Alberta Environment and Sustainable Resource Development, and the NT Government for their logistical support during fieldwork. We are grateful to Neil G. Loader (Swansea University) for help with the carbon analysis.

References

Alexander ME, Stefner CN, Mason JA *et al.* (2004) Characterizing the Jack Pine - Black Spruce Fuel Complex of the International Crown Fire Modelling Experiment (ICFME). Canadian Forest Service, Northern Forestry Centre, report NOR-X-393.

Alexis MA, Rase DP, Rumpel C *et al.* (2007) Fire impact on C and N losses and charcoal production in a scrub oak ecosystem. *Biogeochemistry*, **82**, 201–216.

Aponte C, Tolhurst KG, Bennett L (2014) Repeated prescribed fires decrease stocks and change attributes of coarse woody debris in a temperate eucalypt forest. *Ecological Applications*, **24**, 976–989.

Bird MI, Ascough PL (2012) Isotopes in pyrogenic carbon: a review. *Organic Geochemistry*, **42**, 1529–1539.

Boden TA, Marland G, Andres RJ (2012) *Global, Regional, and National Fossil-Fuel CO2 Emissions*. Department of Energy, Carbon Dioxide Information Analysis Center, Oak Ridge National Laboratory, Oak Ridge, Tenn., USA.

Bodí MB, Martin DA, Balfour VN *et al.* (2014) Wildland fire ash: production, composition and eco-hydro-geomorphic effects. *Earth-Science Reviews*, **130**, 103–127.

Bond-Lamberty B, Scott DP, Ahl DE, Gower ST (2007) Fire as the dominant driver of central Canadian boreal forest carbon balance. *Nature*, **450**, 89–92.

Bowman DMJS, Balch JK, Artaxo P *et al.* (2009) Fire in the earth system. *Science*, **324**, 481–484.

Brewer N, Smith AMS, Hatten JA, Higuera PE, Hudak AT, Ottmar RG, Tinkham WT (2013) Fuel moisture influences on fire-altered carbon in masticated fuels: an experimental study. *Journal of Geophysical Research: Biogeosciences*, **118**, 30–40.

Brown JK (1974) Handbook for inventorying downed woody material. US Dep. Agric., For. Serv., Intermt. For. Range Exp. Stn., Ogden, UT, USA. Gen. Tech. Rep. INT-16.

Carvalho EO, Kobziar LN, Putz FE (2011) Fire ignition patterns affect production of charcoal in southern forests. *International Journal of Wildland Fire*, **20**, 474–477.

Clark JS, Lynch J, Stocks BJ, Goldammer JG (1998) Relationships between charcoal particles in air and sediments in west-central Siberia. *The Holocene*, **8**, 19–29.

Clay GD, Worrall F (2011) Charcoal production in a UK moorland wildfire - How important is it? *Journal of Environmental Management*, **92**, 676–682.

Cornwell WK, Cornelissen JHC, Allison SD *et al.* (2009) Plant traits and wood fates across the globe: rotted, burned or consumed? *Global Change Biology*, **15**, 2431–2449.

Czimczik CI, Preston CM, Schmidt MWI, Werner RA, Schulze ED (2002) Effects of charring on mass, organic carbon, and stable carbon isotope composition of wood. *Organic Geochemistry*, **33**, 1207–1223.

Czimczik CI, Preston CM, Schmidt MWI, Schulze ED (2003) How surface fire in Siberian Scots pine forests affects soil organic carbon in the forest floor: stocks, molecular structure, and conversion to black carbon (charcoal). *Global Biogeochemical Cycles*, **17**, 1020.

Delisle GP, Woodard PM (1988) Constants for calculating fuel loads in Alberta. Can. For. Serv., North. For. Cent., Edmonton, AB, Canada. For. Manage. Note 45

Donato DC, Campbell JL, Fontaine JB, Law BE (2009) Quantifying char in postfire woody detritus inventories. *Fire Ecology*, **5**, 104–115.

Eckmeier E, Rosh M, Ehrmann O, Schmidt MWI, Schier W, Gerlach R (2007) Conversion of biomass to charcoal and the carbon mass balance from a slash-and-burn experiment in a temperate deciduous forest. *The Holocene*, **17**, 539–542.

Efron B (1982) *The Jacknife, the Bootstrap and Other Resampling Plans*. Society for Industrial and Applied Mathematics, Philadelphia.

Fearnside PM, Leal N, Fernandes FM (1993) Rain-forest burning and the global carbon budget – Biomass, combustion efficiency, and charcoal formation in the Brazilian Amazon. *Journal of Geophysical Research-Atmospheres*, **98**, 16733–16743.

Fearnside PM, Gráça PMLA, Filho NL, Rodrigues FJA, Robinson JM (1999) Tropical forest burning in Brazilian Amazonia: measurement of biomass loading, burning efficiency and charcoal formation at Altamira, Pará. *Forest Ecology and Management*, **123**, 65–79.

Fearnside PM, Gráça PMLA, Rodrigues FJA (2001) Burning of Amazonian rainforests: burning efficiency and charcoal formation in forest cleared for cattle pasture near Manaus, Brazil. *Forest Ecology and Management*, **146**, 115–128.

Fearnside PM, Barbosa RI, Gráça PMLA (2007) Burning of secondary forest in Amazonia: biomass, burning efficiency and charcoal formation during land preparation for agriculture in Apiaú, Roraima, Brazil. *Forest Ecology and Management*, **242**, 678–687.

Finkral AJ, Evans AM, Sorensen CD, Affleck DLR (2012) Estimating consumption and remaining carbon in burned slash piles. *Canadian Journal of Forest Research*, **42**, 1744–1749.

Flannigan M, Cantin AS, de Groot WJ, Wotton M, Newbery A, Gowman LM (2013) Global wildland fire season severity in the 21st century. *Forest Ecology and Management*, **294**, 54–61.

Forbes MS, Raison RJ, Skjemstad JO (2006) Formation, transformation, and transport of black carbon (charcoal) in terrestrial and aquatic ecosystems. *Science of the Total Environment*, **370**, 190–206.

Goforth BR, Graham RC, Hubbert KR, Zanner CW, Minnich RA (2005) Spatial distribution and properties of ash and thermally altered soils after high-severity forest fire, southern California. *International Journal of Wildland Fire*, **14**, 343–354.

Gráça PMLA, Fearnside PM, Cerri CC (1999) Burning of Amazonian forest in Ariquemes, Rondonia, Brazil: biomass, charcoal formation and burning efficiency. *Forest Ecology and Management*, **120**, 179–191.

de Groot WJ, Pritchard JM, Lynham TJ (2009) Forest floor fuel consumption and carbon emissions in Canadian boreal forest fires. *Canadian Journal of Forest Research*, **39**, 367–382.

de Groot WJ, Cantin AS, Flannigan MD, Soja AJ, Gowman LM, Newbery A (2013) A comparison of Canadian and Russian boreal forest fire regimes. *Forest Ecology and Management*, **294**, 23–34.

IPCC (2013) Working Group I Contribution to the IPCC Fifth Assessment Report Climate Change 2013: The Physical Science Basis (Final Draft Underlying Scientific-Technical Assessment).

Kane ES, Hockaday WC, Turetsky MR, Masiello CA, Valentine DW, Finney BP, Baldock JA (2010) Topographic controls on black carbon accumulation in Alaskan black spruce forest soils: implications for organic matter dynamics. *Biogeochemistry*, **100**, 39–56.

Kauffman JB, Cummings DL, Ward DE, Babbitt R (1995) Fire in the Brazilian Amazon 1. Biomass, nutrient pools and losses in slashed primary forests. *Oecologia*, **104**, 397–408.

Kauffman JB, Cummings DL, Ward DE (1998) Fire in the Brazilian Amazon 2. Biomass, nutrient pools and losses in cattle pastures. *Oecologia*, **113**, 415–427.

Kelly R, Chipman ML, Higuera PE, Stefanova I, Brubaker LB, Hu FS (2013) Recent burning of boreal forests exceeds fire regime limits of the past 10 000 years. *Proceedings of the National Academy of Sciences of USA*, **110**, 13055–13060.

Knorr W, Lehsten V, Arneth A (2012) Determinants and predictability of global wildfire emissions. *Atmospheric Chemistry and Physics*, **12**, 6845–6861.

Kuhlbusch TAJ, Crutzen PJ (1995) Toward a global estimate of black carbon in residues of vegetation fires representing a sink of atmospheric CO_2 and source of O_2. *Global Biogeochemical Cycles*, **9**, 491–501.

Kuhlbusch TAJ, Crutzen PJ (1996) Black carbon, the global carbon cycle, and atmospheric carbon dioxide. In *Biomass Burning and the Global Change*. (ed. Levine JS). pp. 160–169. MIT Press, Cambridge, MA, USA.

Kuhlbusch TAJ, Andreae MO, Cachier H, Goldammer JG, Lacaux JP, Shea R, Crutzen PJ (1996) Black carbon formation by savanna fires: measurements and implications for the global carbon cycle. *Journal of Geophysical Research*, **110**, D19, 23,651–23665.

Lal R (2008) Black and buried carbons' impacts on soil quality and ecosystem services. *Soil & Tillage Research*, **99**, 1–3.

Lehmann J, Skjemstad J, Sohi S *et al.* (2008) Australian climate–carbon cycle feedback reduced by soil black carbon. *Nature Geosciences*, **1**, 832–835.

Lynch JA, Clark JS, Stocks BJ (2004) Charcoal production, dispersal, and deposition from the Fort Providence experimental fire: interpreting fire regimes from charcoal records in boreal forests. *Canadian Journal of Forest Research*, **34**, 1642–1656.

Makoto K, Kamata N, Kamibayashi N, Koike T, Tani H (2012) Bark-beetle-attacked trees produced more charcoal than unattacked trees during a forest fire on the Kenai Peninsula, Southern Alaska. *Journal of Forest Research*, **27**, 30–35.

Marschner B, Brodowski S, Dreves A *et al.* (2008) How relevant is recalcitrance for the stabilization of organic matter in soils? *Journal of Plant Nutrition and Soil Science*, **171**, 91–110.

Mitchell K (2007) Quantitative analysis by the point-centered quarter method. Hobart and William Smith Colleges. Available at: http://arxiv.org/pdf/1010.3303.pdf (accessed on 03 07 2014).

Moss RH, Edmonds JA, Hibbard KA *et al.* (2010) The next generation of scenarios for climate change research and assessment. *Nature*, **463**, 08823.

Nalder IA, Wein RW, Alexander ME, de Groot W (1999) Physical properties of dead and downed round-wood fuels in the boreal forests of western and northern Canada. *International Journal of Wildland Fire*, **9**, 85–99.

Ohlson M, Tryterud E (2000) Interpretation of the charcoal record in forest soils: forest fires and their production and deposition of macroscopic charcoal. *The Holocene*, **10**, 519–525.

Ohlson M, Dahlberg B, Okland T, Brown KJ, Halvorsen R (2009) The charcoal carbon pool in boreal forest soils. *Nature Geosciences*, **2**, 692–695.

Ottmar RD (2014) Wildland fire emissions, carbon and climate: modeling fuel consumption. *Forest Ecology and Management*, **317**, 41–50.

Pingree MRA, Homann PS, Morrissett B, Darbyshire R (2012) Long and short-term effects of fire on soil charcoal of a conifer forest in southwest Oregon. *Forests*, **3**, 353–369.

Pitkänen A, Lehtonen H, Huttunen P (1999) Comparison of sedimentary microscopic charcoal particle records in a small lake with dendrochronological data: evidence for the local origin of microscopic charcoal produced by forest fires of low intensity in eastern Finland. *The Holocene*, **9**, 559–567.

Preston CM, Schmidt MWI (2006) Black (pyrogenic) carbon: a synthesis of current knowledge and uncertainties with special consideration of boreal regions. *Biogeosciences*, **3**, 397–420.

Räisänen T, Athanassiadis D (2013) Basic chemical composition of the biomass components of pine, spruce and birch. Forest Refine, pp. 4. Available at: www.biofuelregion.se/UserFiles/file/Forest%20Refine/1_2_IS_2013-01 31_Basic_chemical_composition.pdf (accessed on 01 08 2014)

Randerson JT, Chen Y, van der Werf GR, Rogers BM, Morton DC (2012) Global burned area and biomass burning emissions from small fires. *Journal of Geophysical Research*, **117**, G04012.

Rayment GE, Lyons DJ (2011) *Soil Chemical Methods: Australasia*. Csiro Publishing, Melbourne. 495 pp.

Reichstein M, Bahn M, Ciais P *et al*. (2013) Climate extremes and the carbon cycle. *Nature*, **500**, 287–295.

Righi CA, Gráça PMLA, Cerri CC, Feigl BJ, Fearnside PM (2009) Biomass burning in Brazil's Amazonian 'arc of deforestation': burning efficiency and charcoal formation in a fire after mechanized clearing at Feliz Natal, Mato Grosso. *Forest Ecology and Management*, **258**, 2535–2546.

Rumpel C, Ba A, Darboux F, Chaplot V, Planchon O (2009) Erosion budget and process selectivity of black carbon at meter scale. *Geoderma*, **154**, 131–137.

Saiz G, Wynn JG, Wurster CM, Goodrick I, Nelson PN, Bird MI (2014) Pyrogenic carbon from tropical savannah burning: production and stable isotope composition. *Biogeosciences Discuss*., **11**, 15149–15183.

Santín C, Doerr SH, Shakesby RA *et al*. (2012) Carbon forms in and sequestration potential from ash deposits from forest fires: a case of study from the 2009 Black Saturday Fires, Australia. *European Journal of Forest Research*, **131**, 1245–1253.

Santín C, Doerr SH, Preston C, Bryant R (2013) Consumption of residual pyrogenic carbon by wildfire. *International Journal of Wildland Fire*, **22**, 1072–1077.

Schmidt MWI, Skjemstad JO, Czimczik CI, Glaser B, Prentice KM, Gelinas Y, Kuhlbusch TAJ (2001) Comparative analysis of black carbon in soils. *Global Biogeochemical Cycles*, **15**, 777–794.

Schmidt MWI, Torn MS, Abiven S *et al*. (2011) Persistence of soil organic matter as an ecosystem property. *Nature*, **478**, 49–56.

Singh N, Abiven S, Torn MS, Schmidt MWI (2012) Fire-derived organic carbon in soil turns over on a centennial scale. *Biogeosciences*, **9**, 2847–2857.

Singh N, Abiven S, Maestrini B, Bird JA, Torn MS, Schmidt MWI (2014) Transformation and stabilization of pyrogenic organic matter in a temperate forest field experiment. *Global Change Biology*, **20**, 1629–1642.

Soucémarianadin LN, Quideau SA, MacKenzie MD, Bernard GM, Wasylishen RE (2013) Laboratory charring conditions affect black carbon properties: a case study from Quebec black spruce forests. *Organic Geochemistry*, **62**, 46–55.

Stocks BJ (1989) Fire behavior in mature jack pine. *Canadian Journal of Forest Research*, **19**, 783–790.

Stocks BJ, Alexander ME, Wotton BM, *et al*. (2004) Crown fire behaviour in a northern jack pine-black spruce forest. *Canadian Journal of Forest Research*, **34**, 1548–1560.

Tinker DB, Knight DH (2000) Coarse woody debris following fire and logging in Wyoming lodgepole pine forests. *Ecosystems*, **3**, 472–483.

Urbanski S (2014) Wildland fire emissions, carbon and climate: emission factors. *Forest Ecology and Management*, **317**, 51–60.

Van der Werf GR, Randerson JT, Giglio L *et al*. (2010) Global fire emissions and the contribution of deforestation, savanna, forest, agricultural, and peat fires (1997–2009). *Atmospheric Chemistry and Physics*, **10**, 11707–11735.

Van Wagner CE (1987) Development and structure of the Canadian Forest Fire Weather Index System. Can. For. Serv., For. Tech. Rep. 35, Ottawa, ON, Canada.

Volkova L, Weston C (2013) Redistribution and emission of forest carbon by planned burning in *Eucalyptus obliqua* (L. Hérit.) forest of south-eastern Australia. *Forest Ecology and Management*, **304**, 383–390.

Woolf D, Amonette JE, Street-Perrott FA, Lehmann J, Joseph S (2010) Sustainable biochar to mitigate global climate change. *Nature Communications*, **1**, 56.

Worrall F, Clay GD, May R (2013) Controls upon biomass losses and char production from prescribed burning on UK moorland. *Journal of Environmental Management*, **120**, 27–36.

Zimmerman M, Bird MI, Wurster C *et al*. (2012) Rapid degradation of pyrogenic carbon. *Global Change Biology*, **18**, 3306–3316.